

High Resolution Spatial Electroluminescence Imaging of Photovoltaic Modules

J.L. Crozier, E.E. van Dyk, F.J. Vorster

Nelson Mandela Metropolitan University

Abstract

Electroluminescence (EL) is a useful solar cell and module characterisation technique as it is fast, non-destructive and sensitive to the effects of shunt and series resistance and recombination parameters. EL is emitted by a solar cell under forward bias and can be detected by a cooled silicon CCD camera in dark conditions. There is a proportional relationship between the intensity of the emitted EL and the applied bias level. The effects of resistive losses like series and shunt resistances are visible as areas of lower intensity in the EL image. These resistive areas can be detected by comparing EL images taken at different applied biases. Other defects like micro-cracks and broken contact fingers are also easily identified in the EL images. These defects can have a significant effect of the performance and longevity of the module.

In this study a single crystalline silicon PV module is characterised using EL techniques. High resolution EL imaging enables defects in the module such as cracks and broken contact fingers to be identified. The voltage dependence of certain defects detected in the module allows the resistive losses in the module to be characterised.

Keywords: Photovoltaic, Electroluminescence, Current-Voltage Characteristics

1. Introduction

1.1. Electroluminescence

Electroluminescence (EL) is a useful solar cell characterisation technique as it is fast, non-destructive and sensitive to the effects of shunt and series resistance and recombination parameters.

The luminescence emitted due to EL is affected by optical, electrical and resistive effects which are difficult to separate from each other in the EL image. A solar cell or LED can be simulated as a device with electrical or optical terminals (Kirchartz et al., 2009). A solar cell receives an optical input in the form of the incoming light and outputs an electrical current. Conversely a LED receives an electrical input resulting in an optical output. EL occurs when a solar cell is forward biased receiving an electrical input and outputs an emission spectrum, but unlike the semiconductor materials used in LEDs the emission spectra from solar cells is not in the visible region of the electromagnetic spectrum.

The relation describing the reciprocity between the inputs and outputs is the external quantum efficiency of the solar cell and the internally applied voltage at the junction. The reciprocity between the EL emission and the cell's quantum efficiency and voltage has been discussed in detail (Rau, 2007). A solar cell under forward bias can be considered as a spatially extended device where each point of the surface has its own local quantum efficiency and local junction voltage. All these points are connected with resistances in a system of parallel connected diodes (Kirchartz et al., 2009).

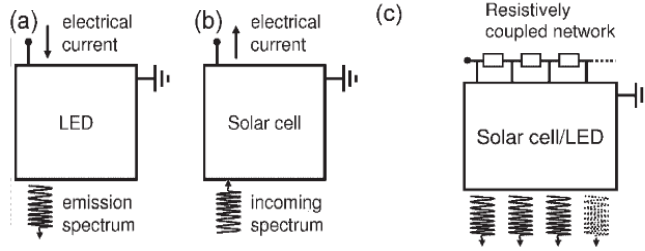


Figure 1: Solar cell represented as a device with optical and electrical terminals (Kirchartz et al., 2009).

1.2. Voltage dependence on EL images

The intensity of the emitted photons is related to recombination mechanisms, material and optical properties of the cell material but there is a strong dependence on the applied voltage. The junction voltage varies across the surface of the cell, but is not wavelength dependant and thus the local junction voltage can be determined from a spatial EL intensity image. Under a constant, stable forward current the intensity of the EL emission of a module can be measured as well as the applied voltage and current. Equation 1 relates the dependence of the local luminescence emission, $\phi(x)$, on the local junction voltage, $V(x)$, at a surface point, x (Potthoff et al., 2010).

$$\phi(x) = C(x) \exp\left(\frac{V(x)}{V_T}\right) \quad (1)$$

This equation holds for conditions where $V(x)$ is much greater than the thermal voltage, $V_T = kT/q$, where k is Boltzmann's constant, T is temperature and q is the charge of an electron. The calibration factor, $C(x)$, is related to optical and material properties of the camera and solar cell. The external applied voltage is equal to the sum of the operating voltages (V_{op}) of the series connected cells in the module. The operating voltage of each cell in a module can be determined from the EL image (Potthoff et al., 2010).

1.3. Spatial high-resolution EL imaging

The photons emitted by EL can be detected by using a cooled Si-CCD camera or alternatively an InGaAs camera. The silicon detector has a lower sensitivity in the longer wavelength range than the InGaAs detector, however, a Si-CCD camera provides better resolution and is less expensive than the InGaAs alternative.

The cooled Si-CCD camera used in this study is sensitive in the 300-1000 nm wavelength range. The peak of the EL emitted by silicon lies outside this region at 1100nm but at exposure times of about 2-3 seconds there is sufficient overlap of the EL signal to obtain a high resolution spatial map of the solar cell.

The camera has a pixel resolution of 3324x2504 or 8.3 MPixel. An EL image of an entire module can be taken if the camera is placed about 1.5 m away from the module. This is ideal for quick defect identification in the module. However, the image resolution is lower and the pixel size is larger. To obtain high resolution images of modules as quickly as possible a motorised system was developed. This involves placing the camera on a motorised carriage and using a LabView programme to move the camera underneath each cell in the module and taking an image. The module and camera are both enclosed in a dark box to prevent any outside light being detected.

1.4. Series and Shunt resistance with reference to dark I-V curves

The I-V curve of a solar cell can be measured in the dark by injecting carriers rather than using photo-generated carriers as in illuminated measurements. This technique is effective in removing subtle variations in the irradiance intensity that can occur in illuminated measurements. In the dark the solar cell behaves like a diode and provides information about the diode factor (n), the saturation current (I_0), series resistance (R_s) and shunt resistance (R_{sh}) of the cell (Hussein et al. 2001). The behaviour of a solar cell in the dark can then be modelled by the dark diode equation:

$$I = I_0 \left[\exp\left(\frac{q}{nkT}(V - IR_s)\right) - 1 \right] + \frac{(V - IR_s)}{R_{sh}} \quad (2)$$

The current-voltage curve can be plotted on a logarithmic axis as shown in figure 2. In the high voltage region a deviation from linear behaviour indicates higher series resistance since at higher voltages high series resistance limits the current. In the low voltage region deviation from linearity indicates high shunt resistance. The curve shapes associated with high and low series and shunt resistance are indicated on figure 2.

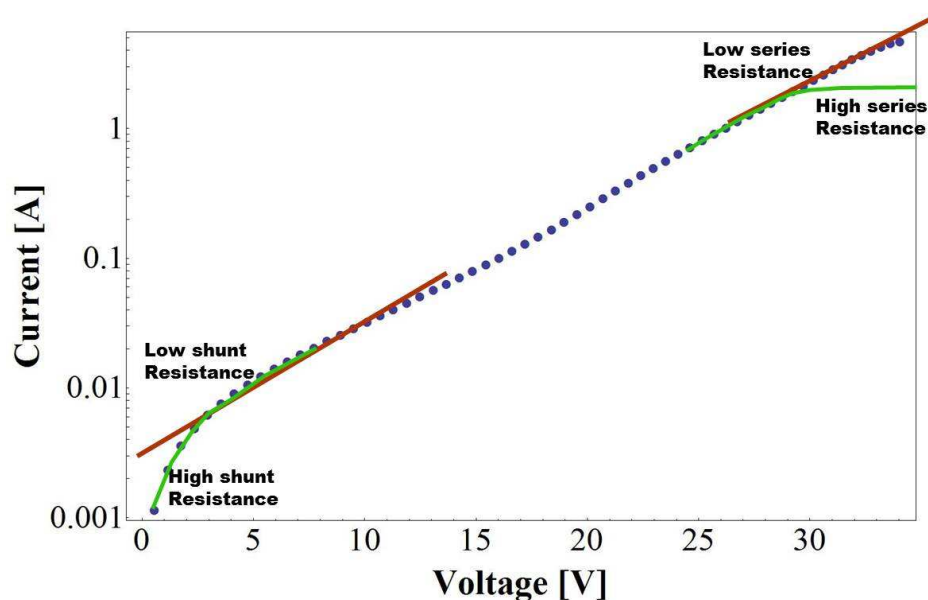


Figure 2: The Dark I-V curve of a PV module on a logarithmic scale.

2. Experimental Procedure

2.1. Equipment

2.1.1. Dark I-V

The Dark I-V system is used to determine the dark current-voltage characteristic of a PV module. The schematic of the components is illustrated in figure 3. The EL and Dark I-V systems share the same power supply and measurement components. Further details of the system components are:

An Agilent E3646A programmable power supply is used for testing single solar cells since it has a range of 8V and 3A. For the higher voltages needed for PV modules the Agilent power supply is used in conjunction with an Elteknix power supply, that has a range of up to 60V and 30A. Agilent 34401A multi-meters are used to measure the voltage across the solar cell or PV module. Another is used to measure the voltage across the shunt resistor and thus determine the current. A GPIB interface between the computer and the equipment

is used to control the applied voltage from the power supply and take readings from the multi-meters. A Labview programme is used to acquire data and plot the current-voltage curve on a log scale. The module is placed in a compartment to ensure completely dark conditions.

2.1.2. Electroluminescence

The modules under investigation are forward biased with current ranging from 10% of the module I_{sc} to greater than the module I_{sc} . The CCD camera is cooled to 50 °C below ambient temperature to improve accuracy and prevent noise in the image from thermally generated carriers in the detector. The exposure time for each image is 3 seconds. The experimental set-up is illustrated in figure 3. The DC power supply forward biases the module to a point, while the applied voltage and current are measured by two digital multi-meters (DMM). The EL image at each applied bias is captured by the camera and stored for further image processing. Combining the EL system with dark I-V system ensures that the applied voltages and currents are accurately measured for each image.

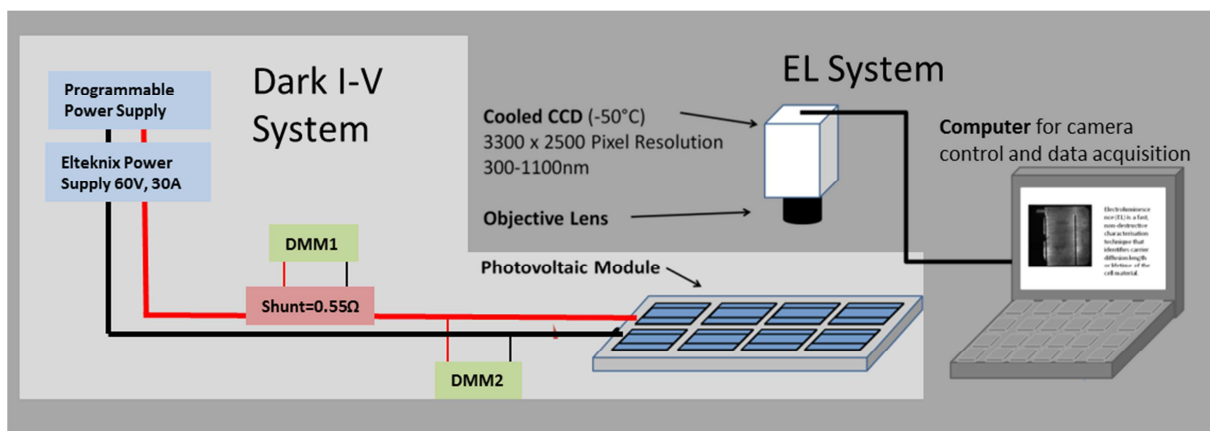
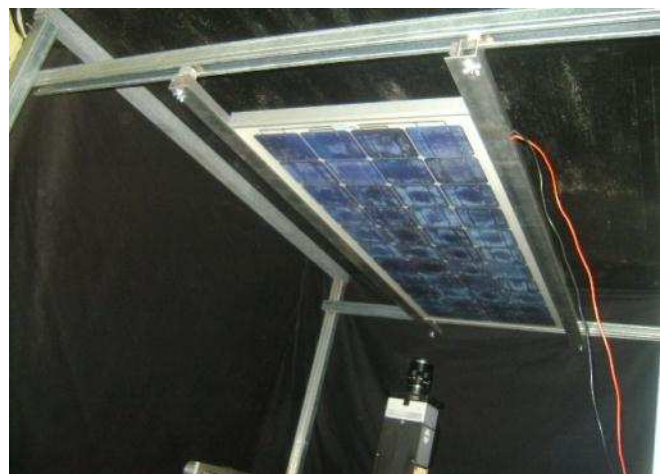


Figure 3: Schematic of EL experimental setup



a)



b)

Figure 4: a) EL camera on motorised carriage, b) position of module to take images of entire module

2.2. Image processing

In order to reduce noise and increase the accuracy all the EL images are processed by removing background noise and erroneous pixels. Firstly a background image is taken under the same conditions as the EL images but without forward biasing the cell. This background image is subtracted from each EL image in order to reduce noise. The images are cropped to the appropriate size and in the case of the high resolution imaging system cell images are compiled together to form an image of the entire module. If quantitative analysis is being done on the images it is important to remove any "bright" pixels. These are pixels that deviate strongly in brightness from their surrounding pixels.

2.3. Outdoor I-V Measurement System

The outdoor I-V measurement system measures the I-V characteristic curve of PV modules in outdoor conditions. The module is placed outside in direct sun conditions and at an optimum testing angle while an electronic load is used to step through a range of voltages allowing the current to be measured at each step. Three digital multi-meters (DMM) are used in the system to ensure accurate module testing. A precision shunt is placed in series with the output current. The voltage across the shunt resistor is measured by DMM 1 and since the resistance of the shunt is known the output current can be determined. The supply voltage is measured using DMM 2 as the electronic load can be inaccurate. DMM 3 is used in conjunction with reference cell or pyranometer to measure irradiance. The function generator is used to simultaneously trigger the electronic load and measurements from the multi-meters. The data collected is relayed to the computer via a GPIB- USB interface.

3. Results

3.1. Images at different applied voltages

In order to discuss the voltage dependence of EL imaging, a 36 cell single crystalline silicon module was tested. Figure 5 shows the optical image of the module and the EL image. The module was not visibly degraded in any way as seen in figure 5(a). The EL image reveals areas of degradation that were not detected in the optical inspection of the module. The module has a short-circuit current (I_{sc}) of 5.5 A and an open-circuit voltage (V_{oc}) of 22.4 V as specified by the manufacturer.

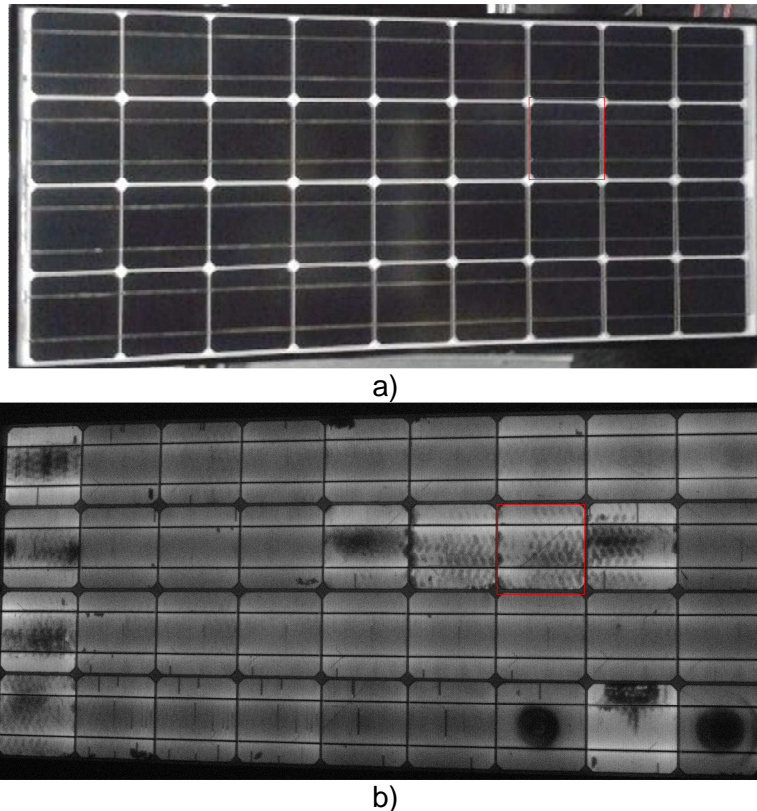


Figure 5: 36 cell single crystalline module, a) optical image and b) EL image. The highlight cell is discussed further.

The cell highlighted in figure 5 is shown in figure 6 at different applied bias levels. The voltage and current bias ranges from a forward current of about 10% of the module I_{sc} to just over 110% I_{sc} . The low intensity signal at a lower current results in an EL image with more noise. From examining the images it is possible to identify defects which are not voltage dependant such as busbars, fingers and micro-cracks. The micro-crack, running diagonally across the cell, is faintly visible even in the low bias image. This indicates that the crack acts a barrier to carrier generation in that region at all voltage levels.

Features that become more prominent at higher bias levels could potentially be related to series resistance. The “tyre track” markings across the cell become more defined and prominent at higher voltage levels potentially relating this defect to regions of higher series resistance. Degradation in the cell material could have occurred during either the cell or module manufacturing process. This degradation increases the series resistance in the affected regions and this series resistance is a limiting factor at higher voltage levels resulting in a lower EL signal. However, further quantitative analysis of the local junction voltage in the affected regions is needed to confirm these assumptions. Shunt resistance effects are visible in a solar cell under low bias voltage conditions. However, since the EL images obtained under low forward bias are not clear it is not possible to visually identify shunts. With refinement in the imaging technique and qualitative analysis, shunted areas in cells should be able to be identified.

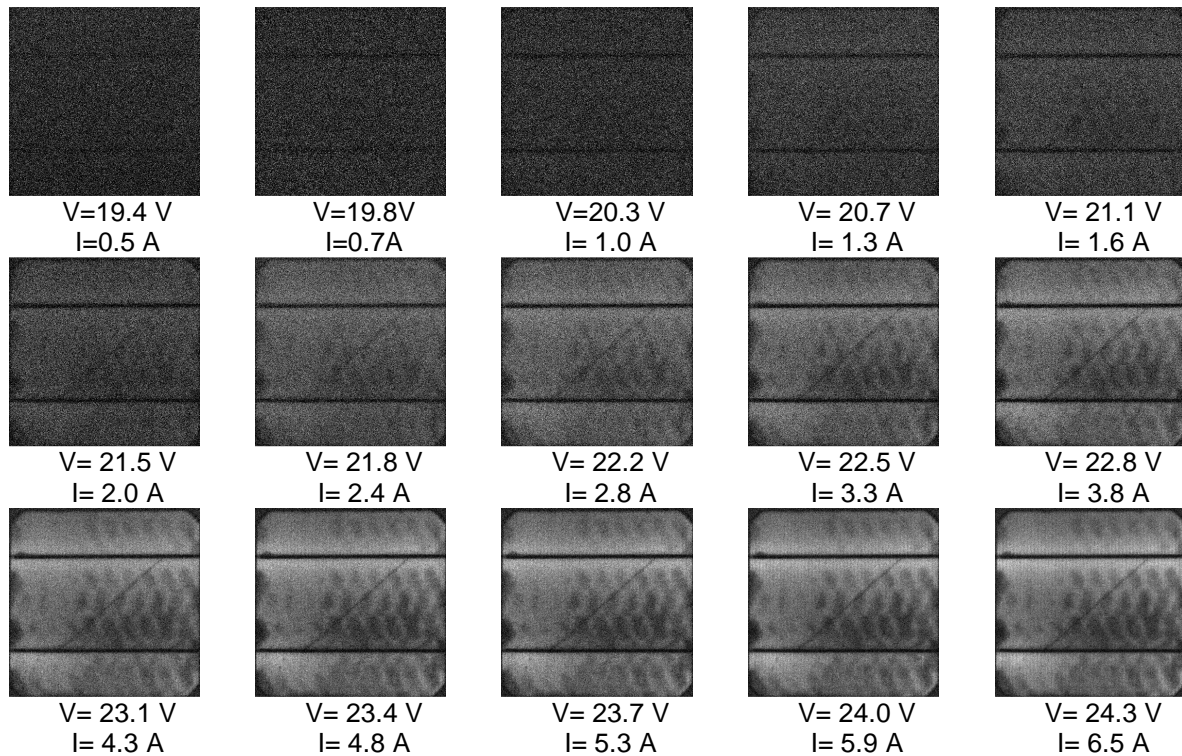


Figure 6: The EL images of a single cell at different bias levels.

3.2. Dark I-V

The dark I-V of the module and the two series connected strings are shown in figure 7. The cells in the module are connected in two strings of 18 cells. String 1 is made up of the top two rows of cells in figure 5 and string 2 is the bottom two. Comparing the dark I-V curves of the two strings allows for some generalised observations to be made about the shunt and series resistance of the cells in the strings. String 1 has lower current in the high voltage region than string 2, indicating a higher series resistance. As can be seen in the EL image in figure 5, string 1 has more degraded cells than string 2 contributing to its higher series resistance. The low voltage region of the curve affected by shunt resistance is the same for both strings indicating similar levels of shunting in both strings.

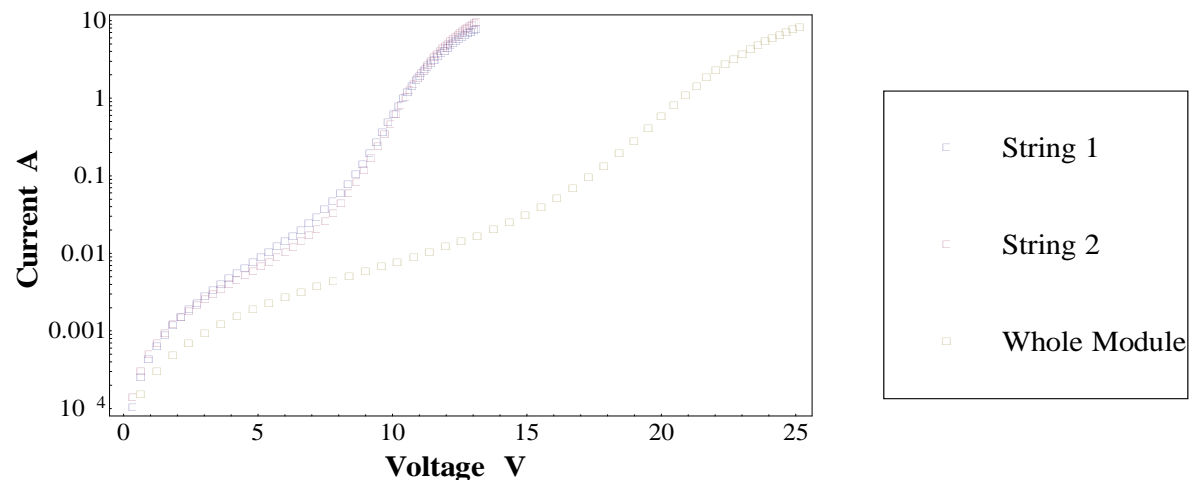


Figure 7: Dark I-V characteristic curves of the individual strings and the whole module.

3.3. Illuminated I-V curve

The illuminated I-V curve of the module and the two strings is shown in figure 8. The two strings are current matched and the whole module produces the manufacturer specified short circuit current of 5.5 A. These results would suggest that the degradation features visible in the EL imaging have very little negative effect on the module performance. However, since this is a brand new module that has no outdoor exposure, the features that were observed could reduce the module performance and increase the degradation over time.

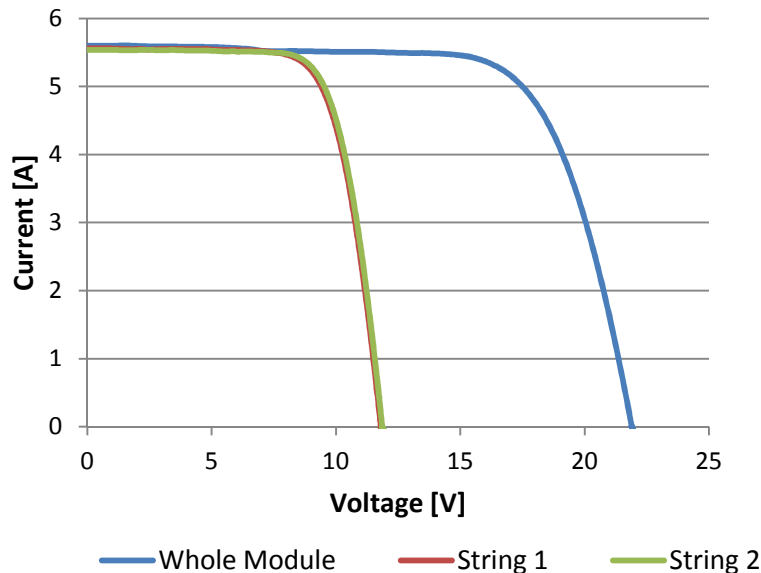


Figure 8: Illuminated I-V curve of the whole module and two strings.

4. Conclusions

EL imaging of PV modules allows some defects and features in the solar cells to be identified. By varying the applied bias voltage further information can be resolved with regard to the resistive losses within the module. The dark I-V characteristic curve is used in conjunction with the EL images to determine the diode behaviour of the module. The EL imaging techniques and the image processing requires further refinement in order to obtain quantitative results like cell operating voltage and series and shunt resistances. These include improving the signal to noise (S/N) ratio of images at low voltage levels and averaging images to improve accuracy. Further improvements in the image processing programme are also necessary to speed up the processing of the high resolution images.

EL images showed defects that were not visible in the visual inspection and did not appear to affect the module performance. Further monitoring of the module in outdoor use could show the long-term effect of these defects on the module performance.

5. References

Hussein R, Borchert D, Grabosch G, Fahrner W.R. 2001. Dark I-V-T measurements and characteristics of (n) a-Si/ (p) c-Si heterojunction solar cells. *Solar Energy Materials & Solar Cells* 69, 123-129.

Kirchartz T, Helbig A, Reetz W, et al. 2009. Reciprocity between electroluminescence and quantum efficiency used for the characterization of silicon solar cells. *Progress in Photovoltaics: Research and Applications*, 17, pp.394-402.

Potthoff T, Bothe K, Eitner U, et al. 2010. Detection of the voltage distribution in photovoltaic modules by electroluminescence imaging. *Progress in Photovoltaics: Research and Applications*, 18, pp.100-106.

Rau U. 2007. Reciprocity relation between photovoltaic quantum efficiency and electroluminescent emission of solar cells. *Physical Review B*, 76, 085303.